BACHELOR

Fatigue in PMMA Copolymers

Kleinjan, Daniël

Award date:
2023

EINDHOVEN UNIVERSITY OF TECHNOLOGY

Bachelor End Project - 4WC00 Quartile 1/2 2022-2023

Fatigue in PMMA Copolymers

Author:
D. Kleinjan 1458388

Supervisor:
prof.dr.ir. L.E. Govaert

January 28, 2023

Contents

1 Introduction

Polymers are increasingly employed in load bearing applications, under difficult environments such as high temperatures or humidities [1]. Therefore, it is important to be able to predict the lifetime of these materials. An issue posed in these type of applications is time dependant failure of polymers, which refers to the fact that under constant load, polymers start to fail at some point. Due to this, it is important to be aware when and how this behaviour occurs.

For the long term performance of polymers, three regions with different failure mechanisms are present. These include plasticity controlled failure, crack growth controlled failure and degradation controlled failure. The first two mechanisms are stress controlled (they are initiated by applied stress) and the latter is caused by chemical circumstances. Is important to notice that these mechanisms act simultaneously until one of them triggers failure [2]. In the plasticity controlled failure region, failure occurs due to an accumulation of plastic deformation which leads to relative ductile failing. In the crack growth failure mode, small cracks in the material start to grow and will eventually become unstable or cause material failure (such as leakage in a pipe). A study shows that these two failure mechanisms and their interaction are generic for a great variety of polymer systems [3]. The last region is the degradation mechanism, which is caused by a chemical reaction and is influenced by the molecular weight of the material. Due to the advances in the chemical industry however, this is not considered to be a limiting material factor anymore [4].

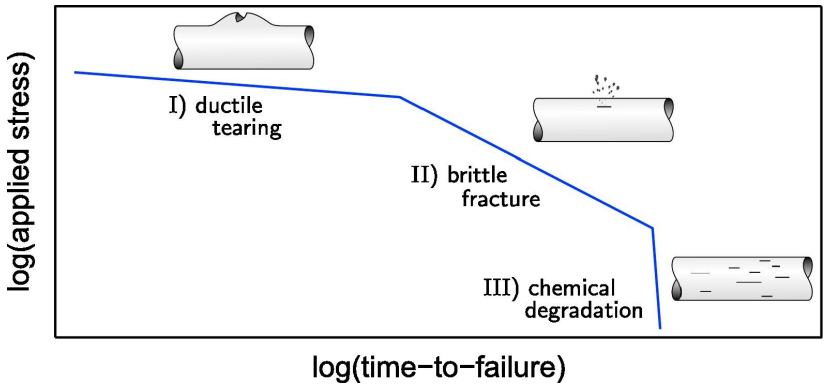

Figure 1: The three failure mechanisms (visualized in a plastic pipe). Reproduced from [5].

To be able to predict the lifetime of polymers, it is not possible to conduct real time experiments, since failure could take decades. As a consequence, fatigue experiments are being employed. In these type of experiments, the material is cyclic loaded under a predefined wave shape, frequency and amplitude. The results of these experiments are then related to static loading conditions, which can tell something about the long term performance [1].

With the upcoming challenges with regards to climate change, material choice for applications is of importance. On top of this, the recycling of materials is essential to prevent waste. Some materials that are being used at the moment will end up as toxic waste after their application. An example of this is issue is windmills. The wings of windmills are produced from glass fibers/epoxy matrix composites, which require heavy and advanced processes to be reused since they cannot be remolded [6]. For this reason, other materials can be considered to replace these composites. A possible successor could be thermoplastics such as Polymethyl-methacrylate (PMMA). This polymer can be reprocessed and a closed loop recycling process can be designed [7].

In this research, two copolymers of PMMA are investigated. The polymers will be subjected to cyclic loading experiments on a constant frequency and stress ratio, with different applied stresses and under varying temperatures. The goal is to define what happens at different temperatures and what failure region occurs.

2 Background

2.1 Plasticity controlled failure

When a polymer experiences stress, molecular mobility is increased [8]. Under constant stress, a continuous plastic flow is caused and at some point, this built up flow leads to failure. This plasticity controlled failure region can be characterized using creep and tensile experiments. Furthermore, an elevated temperature can accelerate the process. This is the consequence of a higher temperature causing more molecular mobility, resulting in more plastic flow [9],[2].

2.1.1 Time to failure prediction

The time to failure within this region is dependent on the stress level. For example, a higher load will lead to more plastic flow, leading to earlier failure. To predict the long term performance of this failure region, a critical strain ε_{cr} (accumulated plastic flow where failure occurs) can be determined. By performing creep experiments at different stresses and capturing both the time to failure (t_f) and the plastic flow rate ($\dot{\varepsilon}_{pl}$) during secondary creep (when the plastic flow increases linearly), a relation can be established to find the critical strain: $\dot{\varepsilon}_{pl} * t_{failure} = \varepsilon_{cr}$. Then, the equation can estimate the time to failure for any stress (if the matching plastic flow rate is known):

$$t_{failure} = \frac{\varepsilon_{cr}}{\dot{\varepsilon}_{pl}} \tag{1}$$

However, instead from experiments, the plastic flow rate can also be calculated by making use of the deformation kinetics in the form of the Eyring flow equation:

$$\dot{\varepsilon}_{pl}(\sigma, T) = \dot{\varepsilon}_0 \exp\left(-\frac{\Delta U}{kT}\right) \sinh\left(\frac{\sigma v^*}{kT}\right) \tag{2}$$

The variables $\dot{\varepsilon_0}$, ΔU and v^* can be determined via fitting data from tensile experiments, based on the strain rate dependence of the yield stress and the influence of different temperatures [2].

For fatigue experiments, the method above is no longer valid. In cyclic loading, the applied stress is not constant anymore but it varies over time, usually as a sinusoidal function where the stress reaches its peaks at the minimum and maximum applied stress. Depending on the maximum stress and the stress ratio, the accumulated plastic strain for one cycle (ε_{apc}) can be determined by integrating the plastic flow over the time of one cycle.

$$\varepsilon_{apc} = \int_0^{t_{\text{cycle}}} \dot{\varepsilon}_{pl}\left(\sigma\left(t'\right), T\right) \mathrm{d}t' \tag{3}$$

Note that the stress and temperature dependence can again be found using the Eyring flow equation.

From experiments, the number of cycles until failure (N_f) can be determined for several maximum applied stresses. By combining this with the plastic flow per cycle and the frequency, the time to failure can be determined [2].

$$t_f = \frac{N_f}{f}\left(= \frac{\varepsilon_{cr}}{f \cdot \varepsilon_{apc}}\right) \tag{4}$$

Moreover, models have been developed to describe this failure region. For example one for creep fatigue life based on low-cycle fatigue experiments [10] or a ratcheting strain model (built up plastic flow during fatigue experiments) for polymers under under wider environmental conditions [11].

2.2 Crack growth controlled failure

In a polymer, there are precursors of cracks. It is the way these initial flaws propagate and eventually become unstable that cause failure. This failure type can be described using Linear Elastic Fracture Mechanics (LEFM) [12]. Using LEFM, the stress field in a crack tip is described using the stress intensity factor K. The value for K depends on the material, crack geometry and the magnitude of the load:

$$K = Y\sigma\sqrt{\pi a} \tag{5}$$

where Y is the geometrical parameter, a is the crack length and σ is the applied stress. At some critical stress value, failure occurs. From this critical stress, the critical stress intensity factor K_{cr} or the fracture toughness, can be found. To describe crack growth, the crack length evolution ($\dot{a}$) needs to be described. To do this, the Paris-Law is employed [13], using the stress intensity factor K and the constants A and m, which are regarded as material parameters:

$$\dot{a} = \frac{da}{dt} = AK^m \tag{6}$$

the value for A refers to the crack propagation rate at $K = 1$ and the value for m, represents the slope of the line. This is visualized in the figure below. Note the log-log scale is used to see the linear relation since the Paris law is a power law.

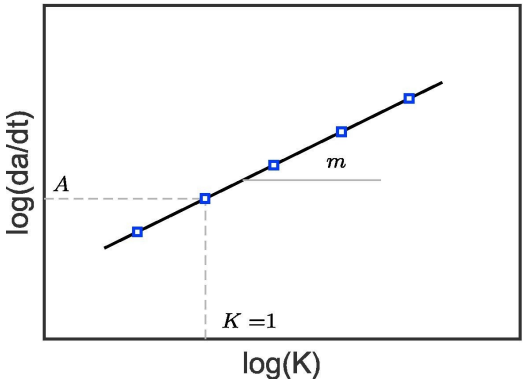

Figure 2: Visualisation of the Paris Law with denoted parameters A and m. Reproduced from [1].

Under static load (creep experiments), the schematic evolution of crack growth can be seen below.

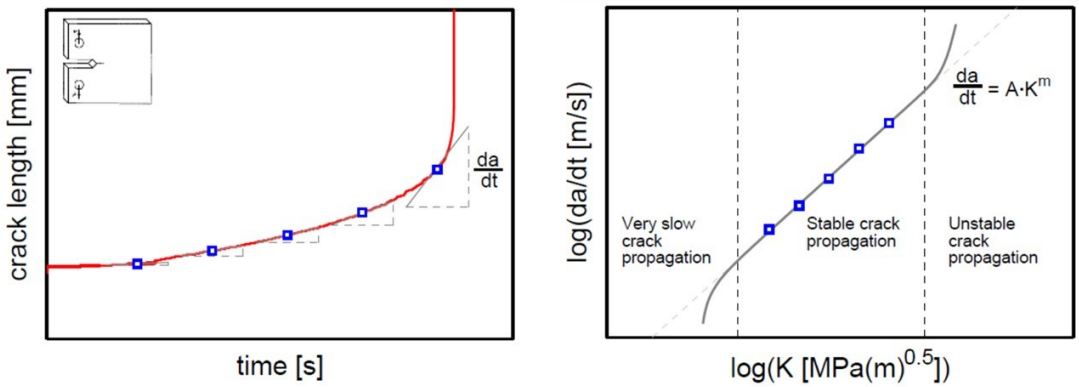

Figure 3: Crack length over time (left) and crack propagation rate over the stress intensity factor K (right). Reproduced from [5].

In a Paris plot, the crack propagation rate is plotted over the fracture toughness. From fatigue experiments, the slope m is also found. The results of these experiments can be plotted in a Wöhler curve and has a negative inverse relation with the slope m from the Paris plot. Note that in a Wöhler curve, the maximum stress is plotted on the y-axis. From now on, when applied stress is mentioned, the maximum applied stress is referred to.

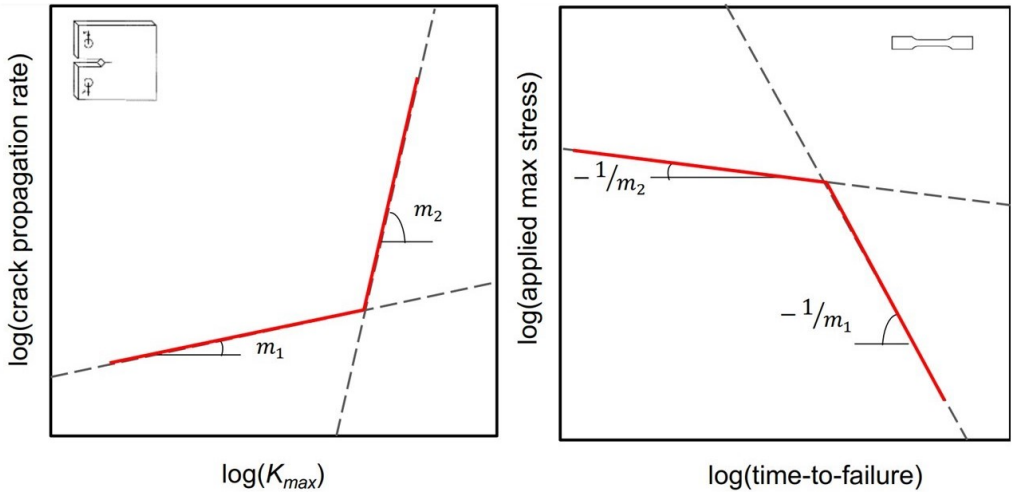

Figure 4: The Paris plot (left) and the Wöhler curve (right).

2.2.1 Time to failure prediction

To be able to predict the time to failure (t_f), the crack propagation rate can be integrated over the initial and final crack length: $t_f = \int_0^{t_f} \dot{a}\, dt$. By rewriting the Paris Law to dt, the following equation is obtained:

$$dt = \frac{da}{AK^m} = \frac{da}{A(Y\sigma\sqrt{\pi a})^m} \tag{7}$$

Filling this into the integral gives a relation to find the time to failure, but also the relation between the applied stress σ and the time to failure:

$$t_f = \left(\frac{1}{A} \int_{a_i}^{a_f} \frac{1}{(Y\sqrt{\pi a})^m} da \right) \cdot \sigma^{-m} \tag{8}$$

where the integral bounds are the initial crack length and the crack length at failure.

$$\sigma = \left(\frac{1}{A} \int_{a_i}^{a_f} \frac{1}{(Y\sqrt{\pi a})^m} da \right)^{\frac{1}{m}} \cdot t_f^{-\frac{1}{m}} \tag{9}$$

Finally, the large part in brackets is often denoted as c_f and can be determined by fitting experimental fatigue data. This results in the simplified equation:

$$\sigma = c_f \cdot t_f^{-\frac{1}{m}} \tag{10}$$

On a double logarithmic scale, equation 10 is a linear relation with slope $-1/m$. From fatigue experiments, an applied stress results in a matching time to failure. From these datapoints, the value for m can be determined using a fitting tool. Additionally, the position (or height) of the curve can be determined, which is related to c_f. This method will be applied to construct the Wöhler curves.

To be able to predict the long term performance of crack growth, real time experiments are not possible because it could take decades until this failure type occurs in a polymer. A model to predict long term crack growth in static loading (creep) was developed by making use of the results from fatigue experiments at different frequencies and stress ratios [1].

2.3 Transition & Distinction

When the transition from static experiments to cyclic experiments under the same applied load is reviewed, the two described mechanisms have a different effect. This effect can be used to identify which mechanism occurs upon failure [3]. Within the plasticity controlled region, the time to failure in a cyclic loading experiment will be longer than in a creep experiment due to the fact that plastic flow accumulates slower and thus failure occurs after more time [2]. For the crack growth region, the opposite is found. Here, the time to failure is shorter for cyclic loading experiments than under static conditions. This phenomenum is the result of the cyclic load component inducing an additional step wise crack propagation, related to fibril failure. In the material, small crazes are present with fibrils spanning between the crack surfaces. When these are loaded and unloaded (which is done by the cyclic motion), they are continuously stretched and crushed/bend, which results in more damage per cycle compared to stretching (static loading) experiments. Therefore, the fibrils fail quicker and a lower lifetime is found [14],[15].

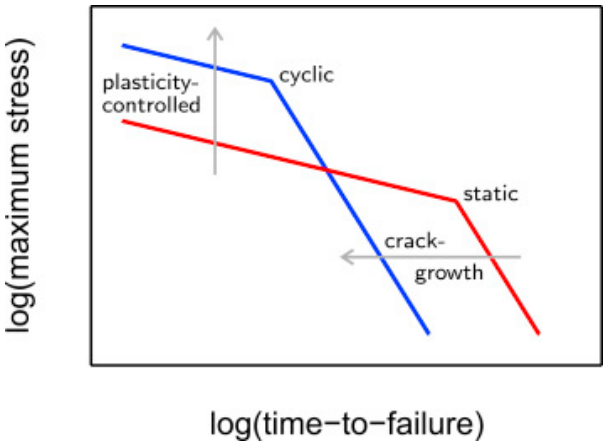

Figure 5: Visualization of the transition from static loading to cyclic loading for the two failure mechanisms. Reproduced from [2].

The influence of varying variables in fatigue experiments has been researched earlier for the different regimes [16]. A notable result was found: in the plasticity controlled regime, the lifetime is independent of frequency. Furthermore, lifetime increases with increasing stress amplitude (or decreasing stress ratio) [17]. In the crack growth regime, the exact opposite is found: higher frequencies result in lower lifetimes. This is related to the above discussed fibril failure phenomenum, only when the frequency is increased, the fibrils are loaded and unloaded even faster because of the higher frequency, which again induces an increase in crack propagation rate and a lower lifetime [14],[15]. In addition, a higher stress amplitude (or lower stress ratio), results in shorter lifetimes [17].

2.4 Activation energy

From fatigue experiments at different temperatures, the activation energy can be calculated using the Arrhenius equation. This is based on how a change in temperature shifts equation 10 and thus causes a change in the rate of a process, which is in this research the crack propagation rate [18].

$$k(T) = A \exp\left(\frac{-\Delta U}{RT}\right) \tag{11}$$

In the Arrhenius equation, k features the process rate (denotes that it is influenced by temperature), A is the pre exponential factor, ΔU is the activation energy, R refers to the universal gas constant and T is the temperature in Kelvin.

By determining a shift factor, which effectively relates to how curve of equation 10 shifts horizontally and thus the process rate changes, the activation energy can be determined. One of the temperatures will be used as a reference temperature to determine the shift factors. This means that the shift relative to the reference temperature curve is the shift factor. This leads to the following simplified equation:

$$a_t = \exp\left(\frac{-\Delta U}{RT}\right) \tag{12}$$

When the exponential is removed from the equation and the natural logarithm of the shift factors are plotted over $1/T$, a linear relation can be established, with slope $\frac{\Delta U}{R}$:

$$log(a_T) = \frac{-\Delta U}{R} \cdot \frac{1}{T} \tag{13}$$

By making use of a fitting tool, the optimal slope can be determined. Then, the activation energy can be determined by multiplying the optimal slope with the universal gas constant R. An important observation to state here is that this specific method is only applicable when the slope of the curves is the same, otherwise the shift factor will be dependant on the location where the horizontal difference is being investigated.

To verify this process, a formula for determining the shift factor based on the activation energy (equation 14) can be used [19]. If the activation energy calculated above is filled in in equation 14 and the same shift factor comes out, the process is verified.

$$a_T(T) = \exp\left(\frac{\Delta U_{\mathrm{a}}}{R}\left(\frac{1}{T} - \frac{1}{T_{\mathrm{ref}}}\right)\right) \tag{14}$$

2.5 PMMA & Copolymerisation

The materials that are being investigated both contain mostly the monomer MMA. PMMA is popular among many applications due to its transparency, light weight, mechanical and weathering resistance and the ability to be easily thermoformed [20]. One of the most popular synthetic methods to produce PMMA is radical polymerization. PMMA powder is produced by suspension polymerization, where tiny droplets of MMA monomer react while being suspended in water and a radical initiator. This results in grains of powder which can be used for extrusion to produce for example sheets of PMMA [21]. In this research, the PMMA is combined with another monomer. When a polymer consists of two (or more) dissimilar repeat units in combination along its molecular chains, it is referred to as a copolymer [22]. This research investigates two copolymers. The first one is PMMA with 4 wt% Ethyl Acrylate (EA) and the second one is PMMA with 4 wt% MAA. This means that 96% of the weight of the copolymer consists of the MMA monomer, where the other 4% is either MAA or EA. The chemical structures of the three monomers can be found below.

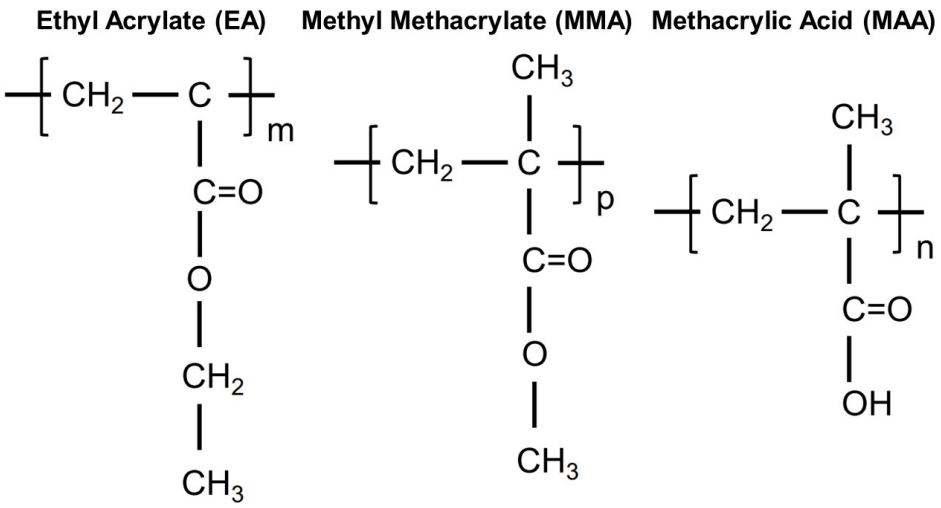

Figure 6: The chemical structures of Ethyl Arcylate, Methyl Methacrylate and Methacrylic Acid.

When comparing a MMA monomer structure with the other two, it can be seen that the EA monomer only has a methyl group at a different location. This change results into a glass transition temperature (T_g) of -23 °C instead of 105 °C for MMA [22],[23]. This is caused by the increased length of the side chain for EA, which causes a decrease in T_g because less chain interactions are possible. For the MAA monomer, a methyl group is replaced with a hydroxy group, creating a carboxyl group at the end of the monomer. Because of this, the monomer can have more dipole interactions. Additionally, the side chain becomes shorter, which can cause more chain interactions. These effects should lead to an increase in T_g, which is indeed the case: for MMA, T_g is 228 °C [2], [23].

2.5.1 Fatigue behaviour PMMA

Fatigue experiments are conducted on PMMA in earlier studies from which the failure mechanism was identified to be crack growth [10],[24]. This can be concluded from the observation that when the frequency is changed, the failure time changes for the same applied stress. This means the lifetime is frequency dependent, which is a known characteristic from the crack growth region as is explained in section 2.3. To see the behaviour of the crack growth region within PMMA, Wöhler curves are employed. This shows that in PMMA, two regions of crack growth can be noticed, each with a different slope or value for $1/m$. For both regions a slope is fitted with either a higher slope of $-1/4$ or lower slope $-1/14$.

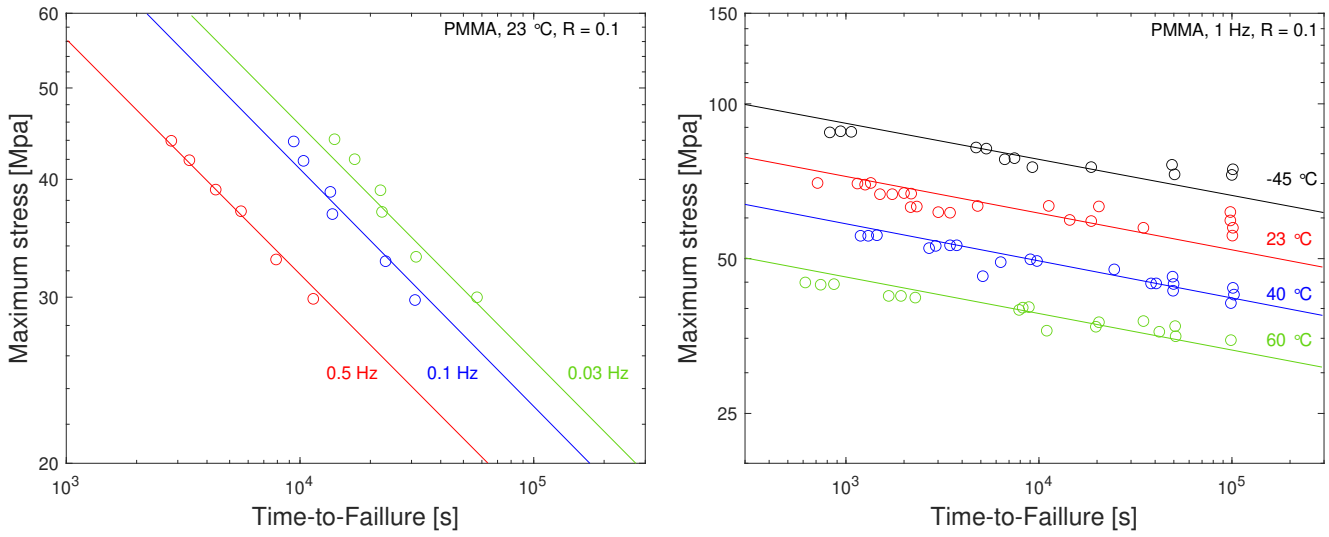

(a) (b)

Figure 7: Experimental data from fatigue experiments with a high slope region and a $-1/4$ fitcurve (a) and a low slope region with a $-1/14$ fitcurve (b). Data reproduced from [10],[24].

It is important to recognize what causes these two failure regions. The region with the high slope, displayed in Figure 7a, shows failure due to growing crazes and fibril failure. Because of chain slip (also called disentanglement) [2], where chains are sliding along each other and lose contact, fibrils in the crazes start to fail, which ultimately results in critical

failure. This process has been elaborated for the thermoplastic high density Polyethylene (HDPE), where the same slope was found as for PMMA in this slope region [25]. Based on a study on PMMA fatigue experiments with this failure region, activation energies of 33, 23 and 17 kJ/mol for frequencies of 1, 10 and 100 Hz were found [26]. Hence, for this research (conducted at 5 Hz), the activation energy is expected to be between 23 and 33 kJ/mol.

The second failure region shows a less steep slope ($-1/14$). When this is the case, the shift factors tend to increase for different temperatures since a lower slope indicates a larger horizontal shift. This can be noticed in Figure 7b. For the same applied stress, the lifetime increases with more than a decade when the temperature is decreased. From previous fracture toughness research on PMMA (displayed in Paris plots) within the same region [27], the shift factors and hence the activation energy can be calculated. From the experimental data of this research, an activation energy of about 85 kJ/mol is found. This activation energy suggests that a viscoelastic response is present [26], which means that there is relaxation and that the crack growth rate decreases, hence the lower slope. The relaxation type that occurs between 80 and 100 kJ/mol is referred to as the β relaxation, which is for PMMA the rotation of one of the side chains around the carbon-carbon bond [28]. Therefore, based on the activation energy, the β relaxation process is expected to be the determining mechanism in this region.

2.5.2 Fatigue behaviour copolymers

From earlier fatigue research conducted by Leon Govaert on the MAA and EA copolymers at 23 °C, the same slope regions from PMMA were found. In Figure 8, the results of his research can be found. The experiments are conducted at two different frequencies. From the data it can be noticed that for two different frequencies, the time to failure at the same applied stress is different. From this observation it can therefore be concluded that both regions are frequency dependent and are hence in the crack growth regime.

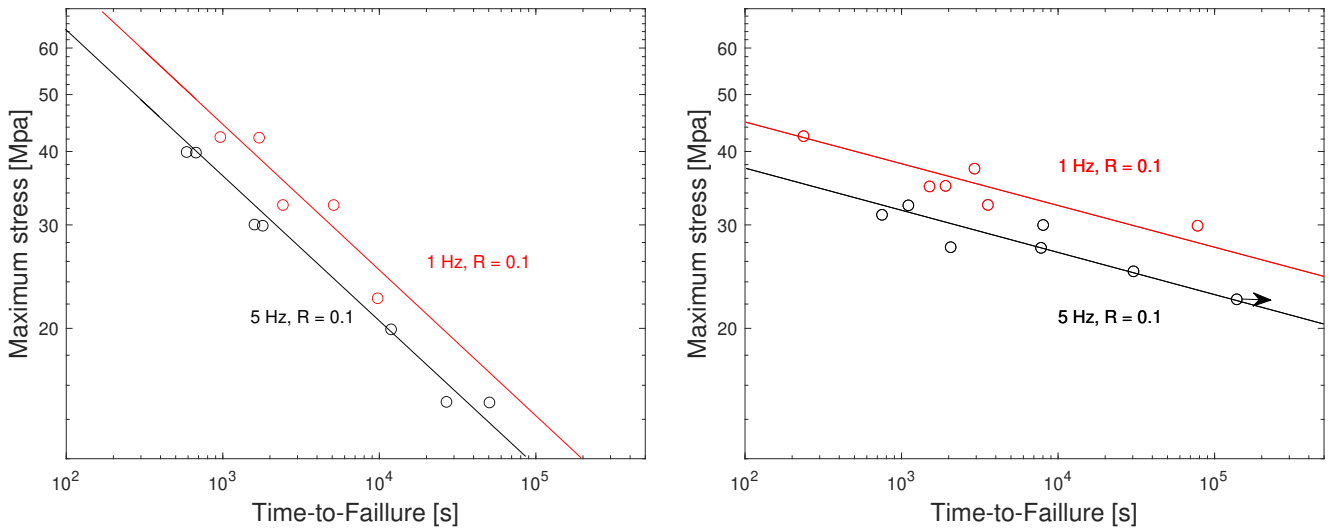

Figure 8: Data from previous research on PMMA-EA fitted with a slope $-1/4$ (a) and PMMA-MAA fitted with a slope of $-1/14$ (b) conducted at room temperature and frequencies of 1 and 5 Hz.

3 Experimental

3.1 Materials

Samples of the copolymers PMMA-MAA (4wt% MAA) and PMMA-EA (4wt% EA) where provided by Trinseo and denotes the samples as HT121 and V825T. The specimen provided have a tensile bar shape and are similar produced, and can be assumed to have the same dimensions.

3.2 Mechanical testing

Fatigue experiments were performed on a servo-hydraulic MTS Testing System and a temperature chamber. Before an experiment was started, the specimen was positioned between the clamps and was aligned to assure the specimen only experiences cyclic motion in the vertical direction. When the experiment was initiated, the stress was first applied to half the maximum stress for 5 seconds. Then, a sinusoidal wave was applied until failure of the specimen where the amount of cycles until failure is used to calculate the time to failure. The frequency of the sinus wave was kept at 5 Hz with a stress ratio of 0.1. For experiments at the temperatures 10 °C and 50 °C, samples were allowed to acclimatize for 15 minutes in the temperature chamber before the experiment was started.

To calculate the maximum force on the specimen during the experiment, the area of the specimen was measured and multiplied with the maximum applied stress. From this, the maximum force is calculated and is inserted in the system to the closest five value (so for a maximum stress of 621.3 N, 620 N is inserted in the system) and the minimum force is taken to be 10% from this value, based on the stress ratio of 0.1.

3.3 Fitting Data

From fatigue experiments, the applied stress functions as the input and the resulting variable is the time to failure. The equation to construct Wöhler curves is defined as follows:

$$\sigma = c_f \cdot t_f^{-\frac{1}{m}} \tag{15}$$

where the variable c_f is the pre-factor and defines the stress that results in a lifetime of 1 s. In Wöhler curves, a double logarithmic scale is used to display the experimental data. Here, the variable $-1/m$ characterizes the slope of the curve.

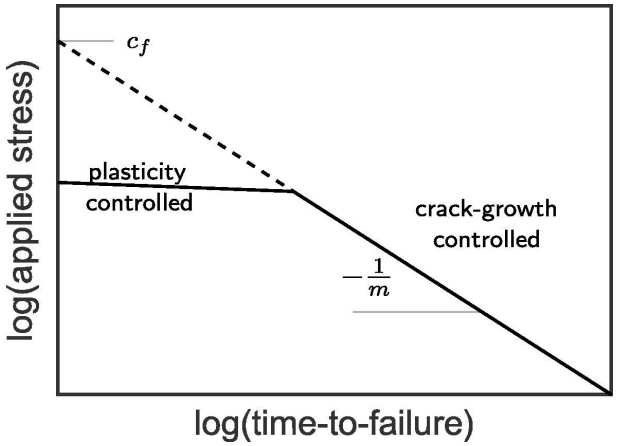

Figure 9: Visualisation of the Wöhler curve with indicated variables. Reproduced from [1].

Note that in this research, only the crack growth regime will be investigated and that the c_f value will be used to fit the height of the curve to the experimental data.

The data from the experiments will be used to fit equation 15. This will be done using the Curve Fitting Tool in MATLAB. The data can be fitted via two ways. The first way is fitting the data while keeping the value $-1/m$ (slope) fixed. This value is based on the data from earlier researches and depending on the copolymer that is researched, this could be $-1/4$ or $-1/14$ [10],[24]. Within this method, the program only fits the value c_f. In the second method, the program will be able to freely choose the best values for $-1/m$ and c_f. This is done to investigate whether the expected slope values from the data of this research, match with these of other researches.

Due to the data being on a double logarithmic scale, equation 15 has a constant slope. Therefore, when the logarithm of the values is taken, the fit has a linear form:

$$y = P1 \cdot x + P2 \tag{16}$$

where x and y are respectively the time to failure and the applied stress. P1 captures the slope and P2 the height of the curve. To relate the P1 and P2 values to the variables m and c_f, the inverse of the log is used, which is 10^x. This gives the following equation that is plotted on a double logarithmic scale, to fit the experimental data. The first component of the equation is the value for c_f and P1 is the value for $1/m$.

$$\sigma = 10^{P2} \cdot t_f^{P1} \tag{17}$$

3.3.1 Fitting methods & Quality analysis

Fitting curves can be done in multiple ways. Within the curve fitting tool of MATLAB, the standard method is least square fitting. This method takes the distance from the fitcurve to each of the data points. Then, the square of the distances is taken and these are summed. This sum is referred to as the sum of deviations. The fitting tool finds the line that has the least summed deviations, which is the best fitting curve [29].

To asses the quality of a fitcurve, the R^2 value can be consulted. This coefficient of determination is a quality indicator that is scale free (which means it does not matter if the data is on a normal scale or on a double logarithmic scale) and denotes the strength of a fit [30]. For every datapoint, the distance to the fitcurve can be calculated. When this is done for every datapoint and this value is squared, the Sum of Squares of the Error term (SSE) is found. On the other hand, the worst fitcurve is a horizontal line. This is when the distances to every datapoints is at its maximum. This is referred to as the Sum of Squares Total (SST) and relates to the worst fit possible. When the SSE is divided by the SST and this value is low, it means that the fit is good since the value is much lower than the maximum error value. To relate this to a value between 0 and 1 the determination coefficient is found [31]:

$$r^2 = 1 - \frac{SSE}{SST} \tag{18}$$

Another quality is the adjusted R^2, which corrects the R^2 when more independent variables are added to the fit. However, since the fit for Wöhler curves only has one independent variable (which is the time to failure), the adjusted R^2 is not necessary.

4 Results

4.1 Experimental results

The results from the conducted experiments on the PMMA-MAA and PMMA-EA copolymers at the temperatures 10 °C, 23 °C and 50 °C can be plotted in Wöhler curves where the maximum applied stress (in MPa) is plotted on the y-axis and the time to failure (in seconds) on the x-axis. The data is plotted on a double logarithmic scale and can be found in Figure 10.

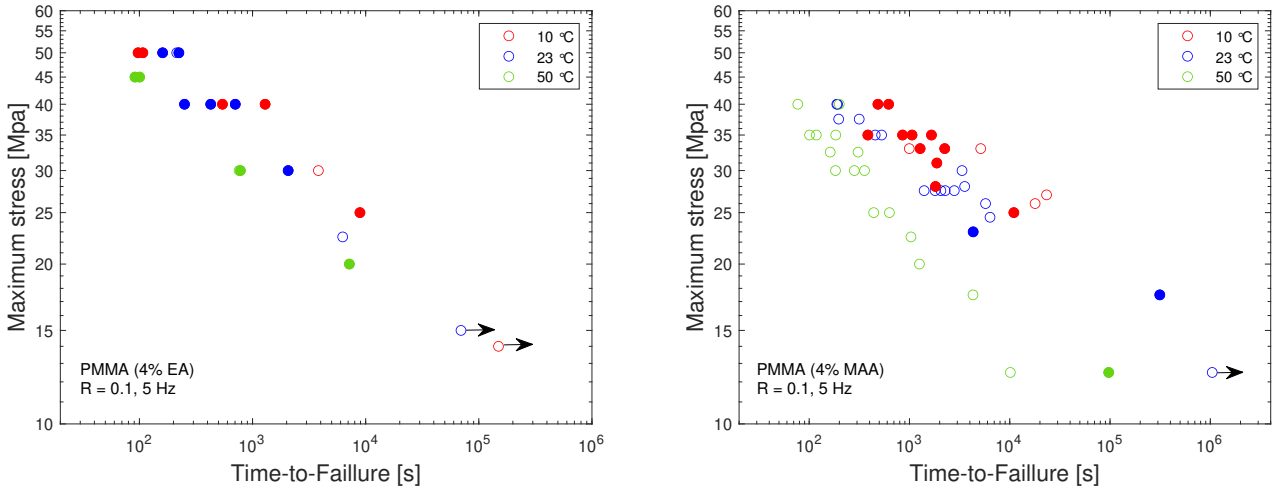

(a) (b)

Figure 10: Data from fatigue experiments conducted on 5 Hz and R = 0.1 at various temperatures for PMMA-EA (a) and PMMA-MAA (b). Open markers indicate failure in the gauge section of the specimen. Filled markers indicate failure at the clamping parts of the specimen. An arrow indicates that the experiment was terminated before failure occurred.

4.2 Comparison to previous research

As mentioned earlier, fatigue experiments on the copolymers researched have been conducted before on room temperature and at the same frequency of 5 Hz. It is useful to compare the two datasets to see whether the results from both researches are coherent. Furthermore, it can verify the quality of the research conducted in this project. Both of the datasets can be found in Figure 11. The lines through the points are the fitcurves that were used to fit the data from the previous research. The fitcurves have a slope of $-1/4$ for the EA copolymer and $-1/14$ for the MAA copolymer. Furthermore, the c_f values of the fits are respectively 200.08 and 51.29.

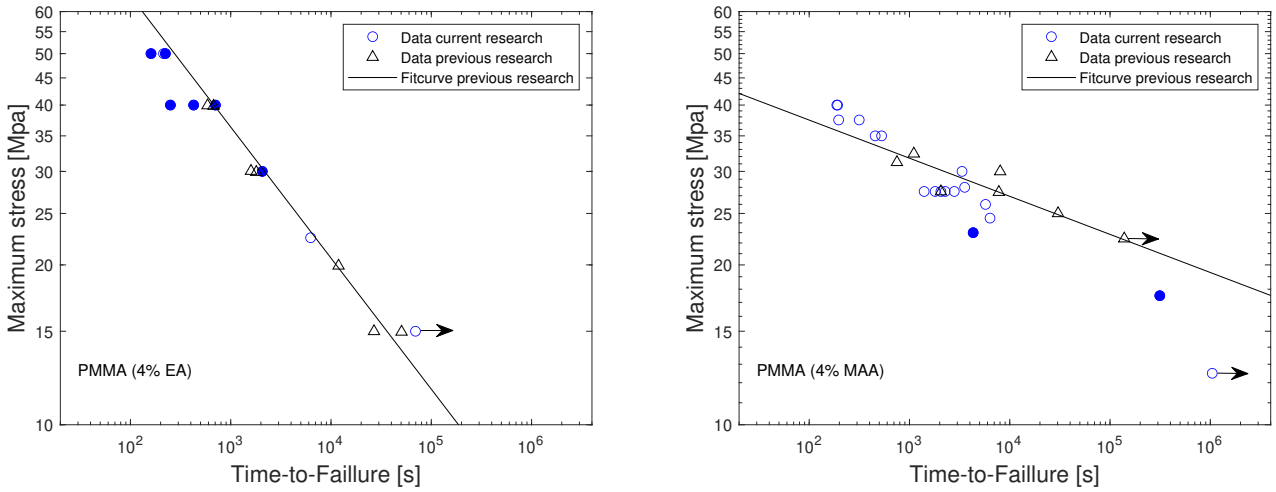

(a) (b)

Figure 11: Data from current and previous research on fatigue experiments on PMMA-EA (a) and PMMA-MAA (b) at 23 °C at 5 Hz and R = 0.1. The fitcurves from previous research with slopes $-1/4$ (a) and $-1/14$ (b) have been used. Open markers indicate failure in the gauge section of the specimen. Filled markers indicate failure at the clamping parts of the specimen. An arrow indicates that the experiment was terminated before failure occurred.

4.3 PMMA-EA fit

The results from the fatigue experiments at the temperatures 10°C, 23°C and 50°C on the PMMA-EA copolymer can be found in Figure 12. The data has been fitted with a predefined slope of $-1/4$, which is based on previous research elaborated in sections 2.5.1 and 2.5.2 and research conducted on PMMA where the same incline was found [10]. The result can be found in Figure 12a. The fit with the free to choose slope can be found in Figure 12b. The parameters for the fitcurves and the quality indicators can be found in Table 1.

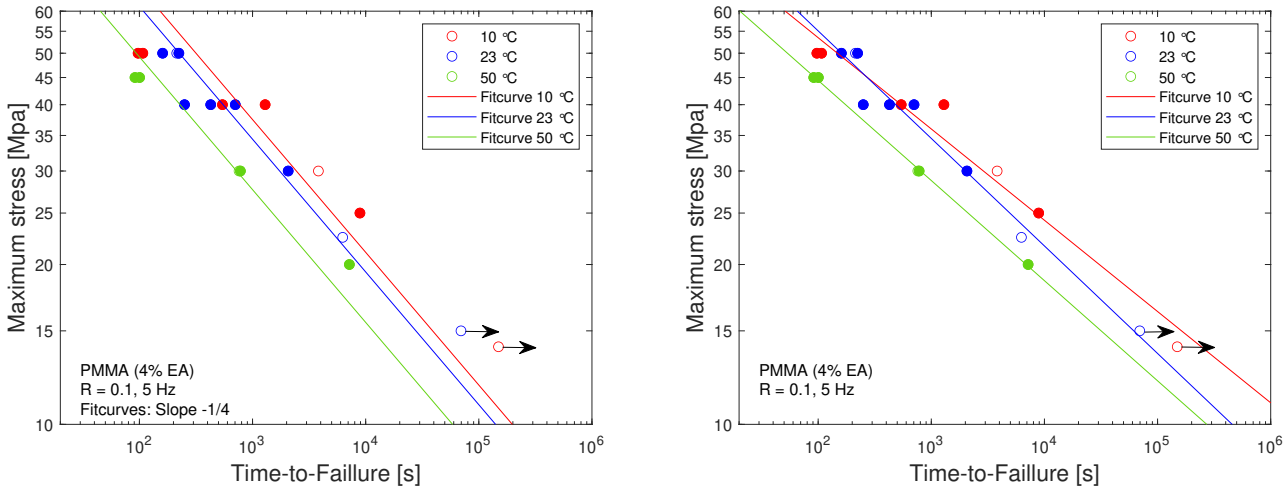

Figure 12: Data from fatigue experiments on PMMA-EA with fitcurves based on the least squares method with a predefined slope (a) and an free to choose slope (b). Open markers indicate failure in the gauge section of the specimen. Filled markers indicate failure at the clamping parts of the specimen. An arrow indicates that the experiment was terminated before failure occurred.

Table 1: Fitting parameters and quality indicators for fatigue experiments on PMMA-EA.

Temperature	Slope $(-1/m)$	Height (c_f)	R^2
Predefined slope fit			
10 °C	-1/4	210.86	0.7682
23 °C	-1/4	193.64	0.9203
50 °C	-1/4	155.60	0.8934
Free to choose slope fit			
10 °C	-0.1719 ($\approx$ 1/ 5.81)	118.03	0.9677
23 °C	-0.2025 ($\approx$ 1/4.94)	139.96	0.9739
50 °C	-0.1886 ($\approx$ 1/5.3)	105.93	0.9992

For the fit with the predefined slope, the shift factors can be determined. In Table 2, the shift factors are denoted. Note that the shift factor for the 23°C is 1, since this is taken as the reference temperature.

Table 2: Values of shift factor a_T from the predefined slope fit on PMMA-EA.

Temperature	Shift factor a_T
10 °C	1.4060
23 °C	1.0
50 °C	0.4168

Plotting the logarithmic shift factors over the inverse temperatures and using the fitting tool to obtain the best slope, the activation energy can be determined. Based on the fit with a R^2 value of 0.9933, the activation energy for the PMMA-EA copolymer is found to be 23.45 kJ/mol.

As explained earlier, equation 14 argues that based on an activation energy value, the matching shift factors can be determined. From this, the method of establishing the activation energy through determining the shift factors can be confirmed. By filling in the found activation energy, one of the shifted temperatures and the reference temperature (23 °C) in equation 14, the two shift factors for 50 °C and 10 °C are found to be respectively 0.4924 and 1.4805.

These values do not exactly match the determined shift factors from Table 2. The reason for this is that based on three shift factors, a fit curve is fitted, which means the activation energy is the average of these three values and therefore they do not exactly match. This however is not an issue since the values are relatively close to each other, concluding that the method does indeed predict the activation energy based on calculated shift factors correctly.

4.4 PMMA-MAA fit

The results from the fatigue experiments at the temperatures 10°C, 23°C and 50°C on the PMMA-MAA copolymer can be found in Figure 13. The data has been fitted with a slope of $-1/14$, which is based on previous research elaborated in sections 2.5.1 and 2.5.2 and the results from research on PMMA where this slope was found as well [24]. The fit parameters and quality indicators can be found in Table 3.

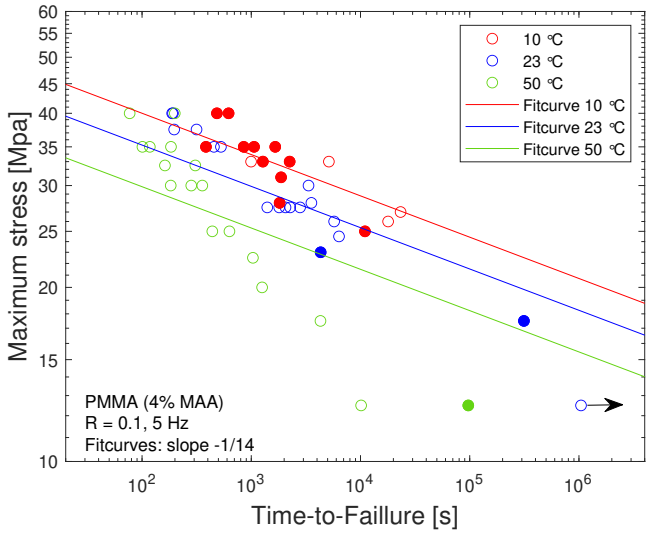

Figure 13: Data from fatigue experiments on PMMA-MAA with fitcurves based on the least squares method with a predefined slope. Open markers indicate failure in the gauge section of the specimen. Filled markers indicate failure at the clamping parts of the specimen. An arrow indicates that the experiment was terminated before failure occurred.

Table 3: Fitting parameters and quality indicators for fatigue experiments on PMMA-MAA.

Temperature	Slope $(-1/m)$	Height (c_f)	R^2
Predefined slope fit			
10 °C	-1/14	55.59	0.6748
23 °C	-1/14	48.98	0.7834
50 °C	-1/14	41.50	0.5638

From Figure 13, it can be noticed that the fitcurves do not follow the the datapoints well, especially at the 50°C datapoints and at 23°C at the lower applied stress datapoints. However, the R^2 values suggest the fits are not great but possible. Although this is the case, when reviewing the datapoints, it looks like if the slope would be steeper from a certain point, more datapoints can be fitted in a better fashion. Furthermore, when comparing the c_f values for this fit at 23 °C and that of the fit from Figure 11b, it can be noticed that it is also too low (51.29 versus 48.98). The fit being lower than expected can be explained by the two lower datapoints that influence the curve negatively and 'pull it down' too much. When assuming a hypothesis of two regions, the second steeper region occurs early in the 50 °C dataset and at a later stage at the 23 °C dataset (for the lowest two datapoints). It is known that this copolymer can show the second steeper region of crack growth, but it was not known until now when this region starts to appear for different temperatures.

The datasets for 50 °C and 10 °C are split into two parts where the first will be fit by means of the first region $(-1/14)$ and the second set will be fit on the second region $(-1/4)$. For the 50 °C dataset, the datapoints of 30 MPa and higher are fitted with the $-1/14$ slope and lower than 30 MPa are fitted with the $-1/4$ slope. For the 10 °C dataset, only the two lowest datapoints (with applied stresses of 17.5 and 12.5 MPa) are fitted with the $-1/4$ slope. The rest of the dataset is fitted with the $-1/14$ slope. The result of this fit can be found in Figure 14. The fit parameters and quality indicators can be found in Table 4.

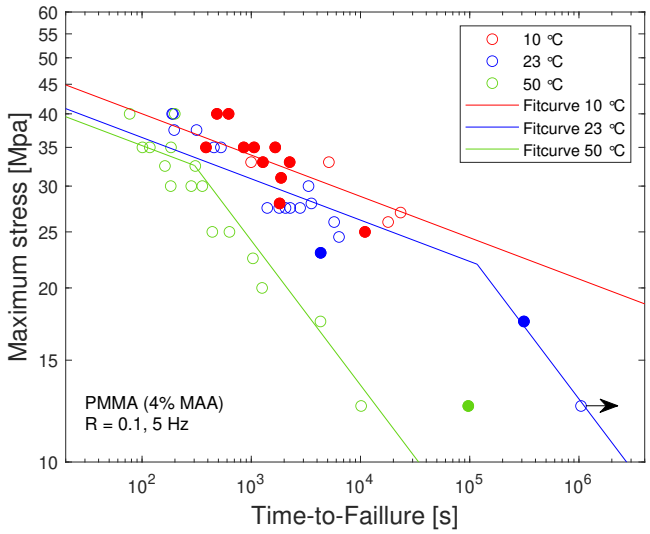

Figure 14: Data from fatigue experiments on PMMA-MAA with two slope regions and fitcurves based on the least squares method. Open markers indicate failure in the gauge section of the specimen. Filled markers indicate failure at the clamping parts of the specimen. An arrow indicates that the experiment was terminated before failure occurred.

Table 4: Fitting parameters and quality indicators for fatigue experiments on PMMA-MMA with two regions.

Temperature	Slope $(-1/m)$	Height (c_f)	R^2
Predefined slope fit - Regime 1			
10 °C	-1/14	55.59	0.6748
23 °C	-1/14	50.58	0.7033
50 °C	-1/14	48.98	0.3161
Predefined slope fit - Regime 2			
23 °C	-1/4	406.44	0.9889
50 °C	-1/4	135.83	0.4397

The determined shift factors for both regions can be found in Table 5. The reference temperature is taken at 23°C.

Table 5: Values of shift factor a_T from the two regions fitting slopes on PMMA-MAA.

Temperature	Shift factor a_T
Region 1	
10 °C	3.7572
23 °C	1
50 °C	0.6358
Region 2	
23 °C	1
50 °C	0.0125

From this, the activation energy for the first low slope region is found to be 31.30 kJ/mol and for the high slope region 129.12 kJ/mol.

5 Discussion

5.1 Experimental conditions & findings

While conducting experiments, it is important to keep the conditions (except the investigated variable condition) similar in order to be able to compare the results correctly. An example is the alignment of the specimen. This means that for every experiment, the clamps and the specimen are aligned so they only experience the cyclic motion in the exact vertical direction. This was done prior to every experiment. One of the factors that could be more difficult to remain similar was the rotational orientation of specimen between the clamps. Before the experiments, it was checked visually whether the specimen was not rotational oriented. Only at later stage a way was found to check this orientation in greater detail, by making use of a bar that was placed against the clamps and kept aligned at one of the clamps. To see whether they are aligned, the other side of the bar should not be able to pivot when pushed.

Another factor that could have influenced the experimental results is a possible difference between input and output of the machine. Before each experiment, a maximum force is inserted into the program that was rounded to the closed five value (for example 622.4 becomes 620 N). This has influenced the output force by a maximum of 2.5 N. Furthermore, when the calibration of the system is off, the expected force could differ from the actual output force. In addition, because of the relatively low stress ratio and high frequency, the system must switch five times a second between for example 1000 N and 100 N. This could be challenging and result in the applied stress not to be exact the requested value. On the other hand, this effect could go both ways so the output could be sometimes too high and sometimes too low, which means this effect could be neglected. Taking these effects together, the calculated force and output force could still be slightly off. This can be investigated by means of an example. Let's say the maximum applied stress is determined to be 25 MPa and the output is 10 N off from the input, the resulting maximum stress is then 24.72 MPa, which is a difference about 1%. For the minimum stress, a difference of 10 N could sound a lot, but it changes the stress ratio to 0.099, which is negligible. From this it can be concluded that these effects can be neglected. Lastly, the offset was not always reset prior to an experiment, hence this could have an influence to the difference between the input and output force.

5.2 Failure at the clamping points

During the conducted experiments, it was found that for some experiments, the failure location was not in the gauge section of the specimen but rather at the ending parts, exactly at the point where the specimen was clamped. The cause for this was expected to be that due to the tightness of the clamps, stress was built up that ultimately lead to quicker failure than the failure initiated by the cyclic motion on the specimen. This meant that for experiments with lower applied stresses and longer lifetimes, failure would occur faster than it should. This made it therefore harder to achieve acceptable results for long term experiments.

In an attempt to prevent this failure from occurring, another set of clamps with a finer structure was used. It was thought that this would lead to less stress localization and prevent the issue from happening. However, this did not solve the problem. It was tried to clamp the specimen less tightly but this often resulted in the specimen coming loose. Consequently, an even finer structure between the clamps and the specimen could possibly solve the issue. This was found in the form of P80 grade sandpaper of which four pieces were used and placed between the clamps at each side where the specimen was in contact with the rough side. This, together with less tight clamping, helped preventing the issue from occurring. Unfortunately this solution was found relatively late in the project and therefore the datasets lack experiments with longer lifetimes. The solution did come with one drawback which was the alignment of the specimen. This became more difficult because of the sandpaper on both sides, which resulted in the upper and lower clamps not being able to be aligned when the specimen was inserted. This was caused by the maximum space between the clamps not being large enough to be adjusted after the specimen and sandpaper were inserted.

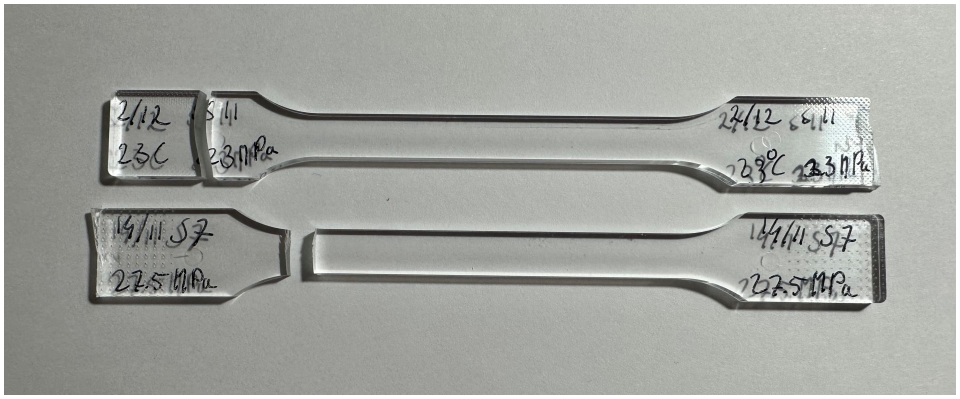

Figure 15: PMMA-MAA specimen failed at clamping part (top) and failed in the gauge section (bottom).

Another possible cause of failing at the the clamping parts could be that at the ends of the specimen, internal stresses cause failure. To investigate whether internal stresses are inside the material, polarisation filters can be used, combined with a light source. The specimen is placed between two polarisation filters under a lamp. If (multiple) colors are observed, it can be concluded that there are internal stresses in the material. This method of investigating the stress field in a material using polarizers is called photoelastic analysis [32]. This has been applied on both copolymers and it was found that there are internal stresses to some degree on the borders of the specimen which could be caused by the manufacturing of the sample. This was the case for the MAA copolymer samples. For the EA copolymer samples, the internal stresses are more spread over the entire specimen. However, for both copolymers, no other colors could be seen, indicating that internal stresses are relatively low. Nevertheless, this method is only based on visual observations and is therefore not completely solid. To investigate this hypothesis, samples could be annealed to reduce internal stresses. In future research, experiments on annealed specimen and normal specimen could be conducted to compare whether failure at the clamping parts occurs more for one of these specimen types.

5.3 Comparison with previous research data

When the comparison between the data from the current research and earlier research is made in Figure 11, it can be noticed that the datasets for the PMMA-EA copolymer give similar results. Only at lower failing times, some datapoints of the current research are a bit off from the fitcurve. These datapoints however show that failure on the clamping parts was observed and that failure in the gauge section would take longer. This could serve as the reason on why these datapoints are more off from the fitcurve based on earlier research.

For the PMMA-MAA copolymer, there is a bit more scatter and some points are more off from the fitcurve presented in Figure 11b. Moreover, for lower applied stresses, something interesting is noticed from the current data. When the failing times increase, failure occurs quicker than expected. This could be explained by the possible second region that occurs and was presented in Figure 14.

5.4 Quality of the fit & Interpretation

When all the datasets were fitted using the MATLAB fitting tool, the values for R^2 were determined based on the standard least square fitting method. However, to investigate whether this was indeed the right method, other methods were explored as well. Based on the quality indicators, it was found that under the least absolute residuals (LAR) method and the Bisquare method, the quality of the fit did not improve significantly, indicating the best method was applied.

5.4.1 PMMA-EA fit

When reviewing the fitcurves of the PMMA-EA copolymer in Figure 12a, it can be noticed that the fits with the predefined curve follow the datapoints well. Additionally, the found activation energy falls into the expected range of fibril failure but at it at the limit. The quality is also confirmed by the quality parameters. However, it can be observed that the 10°C fitcurve is too much to the left. This is also confirmed by it having the lowest R^2 value (0.7682). Furthermore, from the datapoint at 15 MPa, the experiment was terminated before failure occurred, which indicates the failure time would have been longer and the fitting curve should lean more towards this data point. The cause for this is expected to be because of two datapoints (both at 50 MPa), which have a failure time that is significantly lower than the fit (about half a decade). All together, it is interesting to investigate what the result would be if these two datapoints were left out. It is realised that removing datapoints is tricky and that it should be done with caution. However, both of the experiments resulted in failing at the clamping parts, indicating premature failure and hence giving an argument to remove them. The result of the fit without the two datapoints can be found in Figure 16.

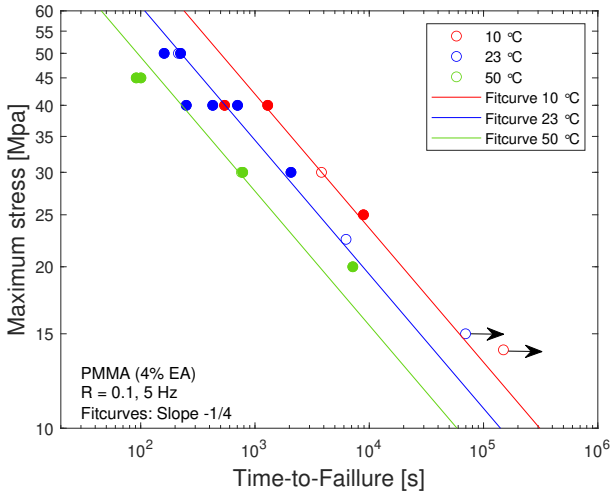

Figure 16: Data from fatigue experiments on PMMA-EA with fitting curves based on the least squares method and an updated fitcurve for 10 °C after removing two datapoints. Open markers indicate failure in the gauge section of the specimen. Filled markers indicate failure at the clamping parts of the specimen. An arrow indicates that the experiment was terminated before failure occurred.

This new fit results a higher R^2 value of 0.9135. The c_f value is 236.05 and the new shift factor has increased to 2.2079. Based on the new shift factor, a new fitcurve is made with a coefficient of determination of 0.9812 which results in an activation energy of 30.99 kJ/mol, which more within the expected region. Additionally, the curve leans more towards the furthest data point which was terminated before failure. These arguments could give the indication that the removal of the two datapoints does increase the quality of the fit.

When comparing the free to choose slope fitcurve to the datapoints presented in Figure 12b, the fit looks a bit better than the initial fit with predefined slope from Figure 12a. This claim is confirmed by the higher R^2 value. Furthermore, it is interesting to see what slopes these curves have, since it can be compared to the slope found in earlier researches. What can be concluded is that the slopes vary between almost 1/5 and 1/6, which means that the slope is a bit less steep than was found in other researches. Moreover, because of the free to choose slope, the fitcurve of 10 °C is a bit to the right of the last datapoint. Because the experiment that belongs to this datapoint was terminated before failure and the point would be further to the right (because failure would have occurred later), this fitcurve follows the dataset well.

5.4.2 PMMA-MAA fit

When comparing the single region fit and the double region fit for the PMMA-MAA copolymer experiments, it can be noticed that due to the second region, more datapoints are better followed. However, the quality of the fit is still not great, which can be noticed from the quality indicators but also from the activation energies, which should be between 80 and 100 kJ/mol for the low slope and between 23 and 33 kJ/mol for the low slope. The low slope region has an activation energy far below this value, with 31.30 kJ/mol and the high slope region has a value that is way higher than what it should be with 129.12 kJ/mol. From this observation it can be concluded that within the low slope region, the curves should be further apart (resulting in a higher activation energy) and for the high slope region, the curves need to be closer to each other (resulting in a lower activation energy).

When reviewing the fitcurves from Figure 14, it is observed that the 10 °C fitcurve should lean more towards the right. This is due to the fact that many of the points have failed at the clamping parts, indicating premature failure which influences the fit negatively. Secondly is the 23 °C dataset. This fitcurve is also too far to the left, indicated by the many points located to the right of the fitcurve. This could be caused by an experiment that has failed on the clamping parts and some experiments that failed too early. For example from the five experiments conducted at 27.5 MPa, four failed too early, which can be said because the fifth point did not fail and there exists a datapoint with a higher applied stress (at 28 MPa) and has a higher lifetime than all datapoints at 27.5 MPa. Moreover, when comparing the c_f value of this dataset to that of previous research, it is still lower (50.58 versus 51.29). For the 50 °C dataset, in the high slope region, there are two results from experiments conducted at 12.5 MPa. One of these is compared to the other much shorter and could therefore influence the fit negatively.

To combine the described aspects that decreased the fit quality, some of the datapoints that have failed too early will be removed, based on the way they failed (on the clamping parts) or that they are too far off from the fitcurve. Again it is noted that this should be done with caution, just as done for the PMMA-EA copolymer fit. The datapoints that will be removed are encircled in Figure 17. The updated fitting curves are presented in Figure 18. The fit parameters and quality indicators are displayed in Table 6.

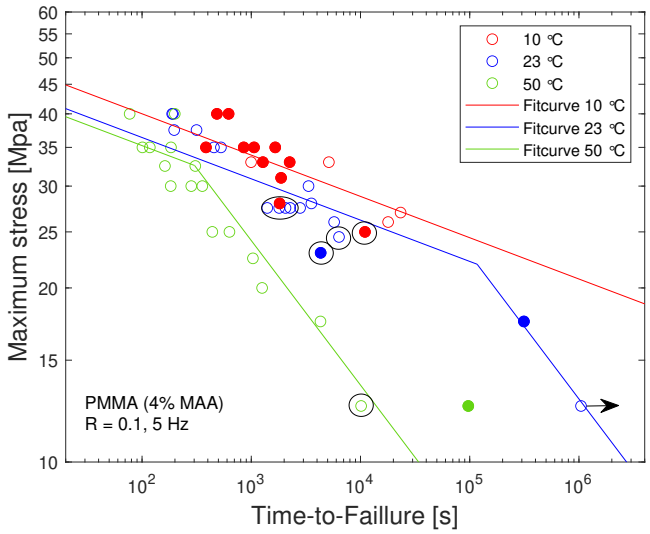

Figure 17: Data from fatigue experiments on PMMA-MAA with indicated datapoints that will be removed.

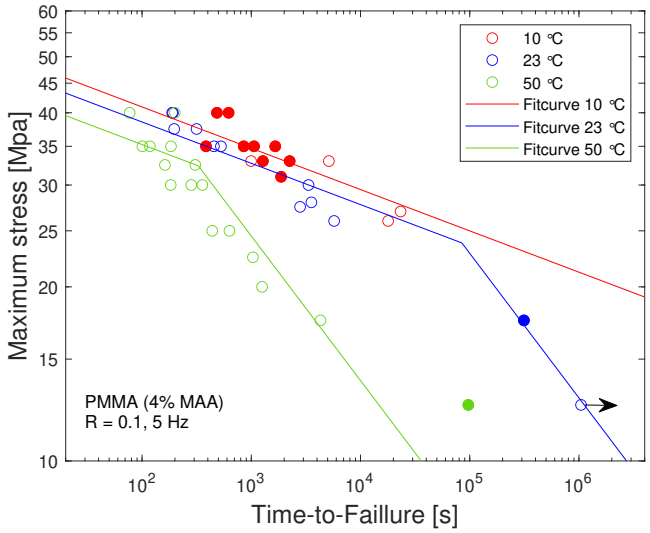

Figure 18: Data from fatigue experiments on PMMA-MAA with two slope regions and updated fitcurves based on the least squares method. Open markers indicate failure in the gauge section of the specimen. Filled markers indicate failure at the clamping parts of the specimen. An arrow indicates that the experiment was terminated before failure occurred.

Table 6: Fitting values and quality indicators for fatigue experiments on PMMA-MAA with two regions and updated fitcurves.

Temperature	Slope $(-1/m)$	Height (c_f)	R^2
Predefined slope fit - Regime 1			
10 °C	-1/14	56.89	0.7562
23 °C	-1/14	53.58	0.8208
50 °C	-1/14	48.98	0.3161
Predefined slope fit - Regime 2			
23 °C	-1/4	406.44	0.9889
50 °C	-1/4	137.72	0.1679

The new shift factors can be found in Table 7. From the updated values, the activation energies for the low slope and high slope regions are respectively 39.59 kJ/mol and 127.54 kJ/mol. It can be concluded that the activation energies from this dataset are still not within the expected range. Furthermore, it should be noted that the activation energy for the low slope region at 50 °C is only based on a single shift factor. Therefore, this value should be noted with

caution. In the ideal world, more experiments on different temperatures would be conducted to achieve more shift factors.

Table 7: Values of shift factor a_T from the updated fitcurves on PMMA-MAA.

Temperature	Shift factor a_T
Region 1	
10 °C	2.3144
23 °C	1
50 °C	0.2835
Region 2	
23 °C	1
50 °C	0.0132

The fitcurves presented in Figure 18 show that the 10 °C fitcurve should still be shifted to the right. However, with the current data this will not be possible, since this dataset contains many clamp failure results. The fit quality of the experiments on 23 °C has increased based on the quality indicator. In addition, compared to previous research, the c_f value is slightly higher. The fit of the 50 °C is still poor and for the high slope region, it became worse. This can be caused by the fact that the datasets contain mostly shorter lifetimes, which results in more scatter than when more experiments with longer lifetimes are conducted. This conclusion is supported by the datapoint at 12.5 MPa, which has a much higher lifetime and failed on the clamping parts, indicating it should have lasted even higher. From more long term testing, the low slope region is expected to stay on longer and hence the transition to the high slope region will occur at lower applied stresses. This will lead to a lower activation energy for the high slope region.

To sum up, even with the better fit, there are still factors influencing the fitcurves negatively, which ultimately result in odd values for the activation energies. The best way to increase the overall quality of the fitcurves is to perform more long term experiments. In general, when comparing the fitcurves of Figures 13 and 18, it is observed that the double region fitcurves follow the datapoints much better than the single region fitcurves and therefore it can be concluded that for the temperatures 23 °C and 50 °C, the second region occurs earlier than initially expected.

5.5 Recommendations

From the analysis of the results, some observations and improvements were suggested to be changed if this project would be done again or follow up research on this topic and these copolymers would be conducted. To improve the conditions of the experiments, the alignment should be optimized. First of all, the rotational alignment based on the bar to rule out that the specimen is rotational oriented is advised. In addition, to prevent premature failure at the clamping parts, clamps with a finer structure should be used and if not possible, P80 grade sandpaper can be used. However, it should be kept in mind that the maximum space between the clamps must be large enough to be able to align the specimen. With these suggestions, the experiments should be easier to execute and result in higher quality data.

As follow up research, more long term data should be gathered on the PMMA-MAA copolymer. With higher lifetimes, the exact transitions to the high slope region could be determined for this copolymer. Furthermore, it is suggested to perform fatigue experiments on more temperatures to improve the quality of the activation energies for both slope regions. Moreover, with the suggestions made to prevent failure at the clamping parts, experiments at 10 °C should be redone since this dataset suffers most from this undesired failure mode. Based on these suggestions, the results from this research could be confirmed or adjusted accordingly to the goal of reaching activation energies that fall in the expected range. Additionally, research into the clamping failure could be conducted. It could be investigated if internal stresses in the specimen are able to initiate the observed premature failure at the clamping parts.

6 Conclusion

In this research, the temperature effects on the time to failure in fatigue experiments were investigated for two copolymers which both show the crack growth failure mechanism. This was based on the observation that they show frequency dependence. It was found that for the copolymer consisting of MMA and EA monomers, all data could be well fitted with a slope of $-1/4$ in a Wöhler curve. When inaccurate datapoints were removed, the quality of the fit increased even more. For this copolymer, an activation energy of 23.45 kJ/mol was found and this increased to 30.99 kJ/mol for the improved fit. These activation energies can be related to the expected failure mechanism of fibril failure which has a range between 23 and 33 kJ/mol, based on the conditions of this experiment.

The experimental data from the PMMA-MAA copolymer shows that for the 23 °C and 50 °C datasets, the second crack growth region appears, instead of the single $-1/14$ region which was expected initially. The fits for this copolymer suffer from more scatter and at the 10 °C temperature experiments, premature failure at the clamping parts was observed. These factors did influence the fit negatively. Based on the best fitcurves, activation energies of 39.59 and 127.54 kJ/mol for the low and high slope region were obtained. Both of these values were off from the expected ranges. The causes for this included the premature failure at the clamping parts and therefore also the lack of more long term experiments. This research presents solutions to overcome this issue in the form clamps with a finer structure and alignment optimizations.

References

[1] Marc J.W. Kanters, Tom A.P. Engels, Tim B. van Erp, and Leon E. Govaert. Predicting long-term crack growth dominated static fatigue based on short-term cyclic testing. *International Journal of Fatigue*, 112:318–327, 7 2018.

[2] Leon E. Govaert, Anne K. Vegt, van der, and Martin. van Drongelen. *Polymers: From Structure to Properties*. Delft Academic Press, 2019.

[3] Marc J.W. Kanters, Takayuki Kurokawa, and Leon E. Govaert. Competition between plasticity-controlled and crack-growth controlled failure in static and cyclic fatigue of thermoplastic polymer systems. *Polymer Testing*, 50:101–110, 4 2016.

[4] Andreas Frank, Pavel Hutař, and Gerald Pinter. Numerical assessment of PE 80 and PE 100 pipe lifetime based on Paris-Erdogan equation. *Macromolecular Symposia*, 311(1):112–121, 1 2012.

[5] M.J.W. Kanters. *Prediction of Long-Term Performance of Load-Bearing Thermoplastics*. PhD thesis, Eindhoven University of Technology, Eindhoven, 2015.

[6] Leon Mishnaevsky, Kim Branner, Helga Petersen, Justine Beauson, Malcolm McGugan, and Bent Sørensen. Materials for Wind Turbine Blades: An Overview. *Materials*, 10(11):1285, 11 2017.

[7] Yasunori Kikuchi, Masahiko Hirao, Takashi Ookubo, and Akinobu Sasaki. Design of recycling system for poly(methyl methacrylate) (PMMA). Part 1: recycling scenario analysis. *International Journal of Life Cycle Assessment*, 19:120–129, 2014.

[8] Hau Nan Lee, Keewook Paeng, Stephen F. Swallen, and M. D. Ediger. Direct measurement of molecular mobility in actively deformed polymer glasses. *Science*, 323(5911):231–234, 1 2009.

[9] C. Bauwens-Crowet, J. M. Ots, and J. C. Bauwens. The strain-rate and temperature dependence of yield of polycarbonate in tension, tensile creep and impact tests. *Journal of Materials Science 1974 9:7*, 9(7):1197–1201, 7 1974.

[10] Aifeng Huang, Weixing Yao, and Fang Chen. Analysis of Fatigue Life of PMMA at Different Frequencies Based on a New Damage Mechanics Model. *Mathematical Problems in Engineering*, 2014:1–8, 2014.

[11] Wei Liu, Zongzhan Gao, and Zhufeng Yue. Steady ratcheting strains accumulation in varying temperature fatigue tests of PMMA. *Materials Science and Engineering A*, 492(1-2):102–109, 9 2008.

[12] T.L. Anderson. *Fracture Mechanics: Fundamentals and Applications*. CRC Press, 3 2017.

[13] P Paris and F Erdogan. A Critical Analysis of Crack Propagation Laws. *Journal of Basic Engineering*, 85(4):528–533, 12 1963.

[14] Ying-Qiu -Q Zhou and Norman Brown. The mechanism of fatigue failure in a polyethylene copolymer. *Journal of Polymer Science Part B: Polymer Physics*, 30(5):477–487, 4 1992.

[15] Y Zhou and N Brown. Anomalous fracture behaviour in polyethylenes under fatigue and constant load. *Journal of Material Science*, 30:6065–6069, 12 1995.

[16] Roel P.M. Janssen, Leon E. Govaert, and Han E.H. Meijer. An analytical method to predict fatigue life of thermoplastics in uniaxial loading: Sensitivity to wave type, frequency, and stress amplitude. *Macromolecules*, 41(7):2531–2540, 4 2008.

[17] Engels T.A.P and L.E. Govaert. Structural Performance of Polymers and their Composites - Lecture Crack-Growth-Controlled failure.

[18] Sergey Vyazovkin. Activation Energies and Temperature Dependencies of the Rates of Crystallization and Melting of Polymers. *Polymers*, 12(5):1070, 5 2020.

[19] Coen C.W.J. Clarijs, Marc J.W. Kanters, Marco J. van Erp, Tom A.P. Engels, and Leon E. Govaert. Predicting plasticity-controlled failure of glassy polymers: Influence of stress-accelerated progressive physical aging. *Journal of Polymer Science, Part B: Polymer Physics*, 57(19):1300–1314, 10 2019.

[20] Sara Babo, Joana Lia Ferreira, Ana Maria Ramos, Anna Micheluz, Marisa Pamplona, Maria Helena Casimiro, Luís M Ferreira, and Maria João Melo. Characterization and Long-Term Stability of Historical PMMA: Impact of Additives and Acrylic Sheet Industrial Production Processes. *Polymers*, 12(10):2198–869, 9 2020.

[21] Raita Goseki and Takashi Ishizone. Poly(methyl methacrylate) (PMMA). In *Encyclopedia of Polymeric Nanomaterials*, pages 1702–1710. Springer Berlin Heidelberg, Berlin, Heidelberg, 2015.

[22] William D. Callister Jr. and David G. Rethwisch. *Materials Science and Engineering*. Wiley, ninth edition, 2018.

[23] Chemical Retrieval on the Web (CROW). Polymer Properties Database - Glass transition temperatures.

[24] Wei Liu, Xuefeng Yao, and Xinwen Chen. A local stress approach to predict the fatigue life of the U-notched PMMA plate at different temperatures. *International Journal of Fatigue*, 103:436–443, 10 2017.

[25] Robin R.J. Cerpentier, Tim van Vliet, Leonid V. Pastukhov, Martin van Drongelen, Mark J. Boerakker, Theo A. Tervoort, and Leon E. Govaert. Fatigue-Crack Propagation of High-Density Polyethylene Homopolymers: Influence of Molecular Weight Distribution and Temperature. *Macromolecules*, 54(24):11508–11521, 12 2021.

[26] W.M. Cheng, G.A. Miller, J.A. Manson, R.W. Hertzberg, and L.H. Sperling. Mechanical behaviour of poly(methyl methacrylate) Part 3: Activation processes for fracture mechanism. *Journal of Materials Science*, 25(4):1931–1938, 4 1990.

[27] G.P. Marshall, L.H. Coutts, and J.G. Williams. Temperature effects in the fracture of PMMA. *Journal of Materials Science*, 9(9):1409–1419, 9 1974.

[28] Johannes Sondhauß, Mark Lantz, and Bernd Gotsmann. β-Relaxation of PMMA: Tip Size and Stress Effects in Friction Force Microscopy. *Langmuir*, 31(19):5398–5405, 2015.

[29] Kumar Molugaram and G. Shanker Rao. Curve Fitting. In *Statistical Techniques for Transportation Engineering*, pages 281–292. Elsevier, 2017.

[30] Sanford Weisberg. Applied Linear Regression. pages 19–46. John Wiley & Sons, Inc., Hoboken, NJ, USA, 1 2005.

[31] G Nieuwenhuis. Statistiek voor het Econasium. Deel II. volume 7, pages 343–354. Unknown Publisher, 2014.

[32] M. M. Shokrieh and A. R.Ghanei Mohammadi. Non-destructive testing (NDT) techniques in the measurement of residual stresses in composite materials: An overview. *Residual Stresses in Composite Materials*, pages 58–75, 2014.